

Image and statistical analysis of melanocytic histology

Jayson Miedema,¹ James Stephen Marron,^{2,3} Marc Niethammer,^{4,5} David Borland,⁶ John Woosley,¹ Jason Coposky,⁶ Susan Wei,² Howard Reisner¹ & Nancy E Thomas^{3,7}

Departments of ¹Pathology and Laboratory Medicine, ²Statistics and Operations Research, ³Lineberger Comprehensive Cancer Center, ⁴Department of Computer Science, ⁵Biomedical Research Imaging Center, ⁶Renaissance Computing Institute and ⁷Department of Dermatology, The University of North Carolina at Chapel Hill, NC, USA

Date of submission 21 June 2011
Accepted for publication 5 December 2011

Miedema J, Marron J S, Niethammer M, Borland D, Woosley J, Coposky J, Wei S, Reisner H & Thomas N E (2012) *Histopathology* 61, 436–444

Image and statistical analysis of melanocytic histology

Aims: We applied digital image analysis techniques to study selected types of melanocytic lesions.

Methods and results: We used advanced digital image analysis to compare melanocytic lesions as follows: (i) melanoma to naevi, (ii) melanoma subtypes to naevi, (iii) severely dysplastic naevi to other naevi and (iv) melanoma to severely dysplastic naevi. We were successful in differentiating melanoma from naevi [receiver operating characteristic area (ROC) 0.95] using image-derived features, among which those related to nuclear size and shape and distance between nuclei were most important. Dividing melanoma into subtypes, even greater separation was obtained (ROC area 0.98 for superficial spreading melanoma; 0.95 for

lentigo maligna melanoma; and 0.99 for unclassified). Severely dysplastic naevi were best differentiated from conventional and mildly dysplastic naevi by differences in cellular staining qualities (ROC area 0.84). We found that melanomas were separated from severely dysplastic naevi by features related to shape and staining qualities (ROC area 0.95). All comparisons were statistically significant ($P < 0.0001$).

Conclusions: We offer a unique perspective into the evaluation of melanocytic lesions and demonstrate a technological application with increasing prevalence, and with potential use as an adjunct to traditional diagnosis in the future.

Keywords: cytometry, image analysis, melanocytic lesions, morphometry, statistical classification

Abbreviations: IRB, internal review board; ROC, receiver operating characteristic

Introduction

Melanoma is a significant cause of morbidity and mortality in the western world, with increasing incidence.¹ The diagnosis and treatment of melanoma and related neoplasms has been described as ‘difficult and dangerous for all concerned’,² and a false negative diagnosis of melanoma is the single most common reason for filing a malpractice claim against a pathol-

ogist.³ A diagnosis of melanoma is made commonly via histological examination of clinically suspicious lesions. However, there are well-known difficulties in differentiating melanoma from benign melanocytic lesions on simple histological examination.⁴ Image analysis uses digital technology to identify and quantitate what the human eye may or may not see, and is a tool that pathologists are likely to utilize increasingly in the future, especially with more frequent digitization of slides.⁵

In current practice, histological analysis is based most commonly on qualitative features as interpreted (sometimes semisubjectively) by a pathologist. Traditional histological features that pathologists look for

Address for correspondence: Professor N E Thomas, MD, PhD, Department of Dermatology, University of North Carolina, 413A Mary Ellen Jones Building, CB 7287, Chapel Hill, NC 27599–7287, USA. e-mail: nancy_thomas@med.unc.edu

differ based on the tissue type at hand. In the context of melanoma, both architectural and cytological features are assessed. In comparison to benign lesions, melanocytic lesions demonstrate disordered architecture, asymmetry and melanocytic epidermotropism (abnormal spreading into the epidermis), as well as cytological pleomorphism and atypia.⁶ Our study concentrated on characterizing cellular (cytometric and morphometric) characteristics and how they compared among different types of melanocytic lesions.

There are many examples in pathology where subjectivity leads to high inter-rater variability. The dermatopathologist is intimately familiar with this type of dilemma, especially in the context of the ongoing arguments over the classification scheme of dysplastic naevi.⁷ This subjectivity complicates patient treatment and is frustrating for clinicians, and for patients who

experience the first-person effects of pathological ambiguity. It is our goal to help to clarify this ambiguity while increasing objectivity and reproducibility.

Technology has changed drastically since the historical development of a large framework of dermatopathological knowledge by Ackerman and others in the last century.^{8,9} Some areas of pathology are increasingly using a combination of computer technology and pathology to make diagnoses. For example, automated quantification has been applied to breast hormone markers¹⁰ and is being employed increasingly by laboratories to facilitate this diagnostic process. The use of image analysis in immunohistochemistry has done much to facilitate decision-making in this area.

In this paper we show that image analysis in conjunction with statistical classification can give deep and useful interpretations. The mind of a well-trained

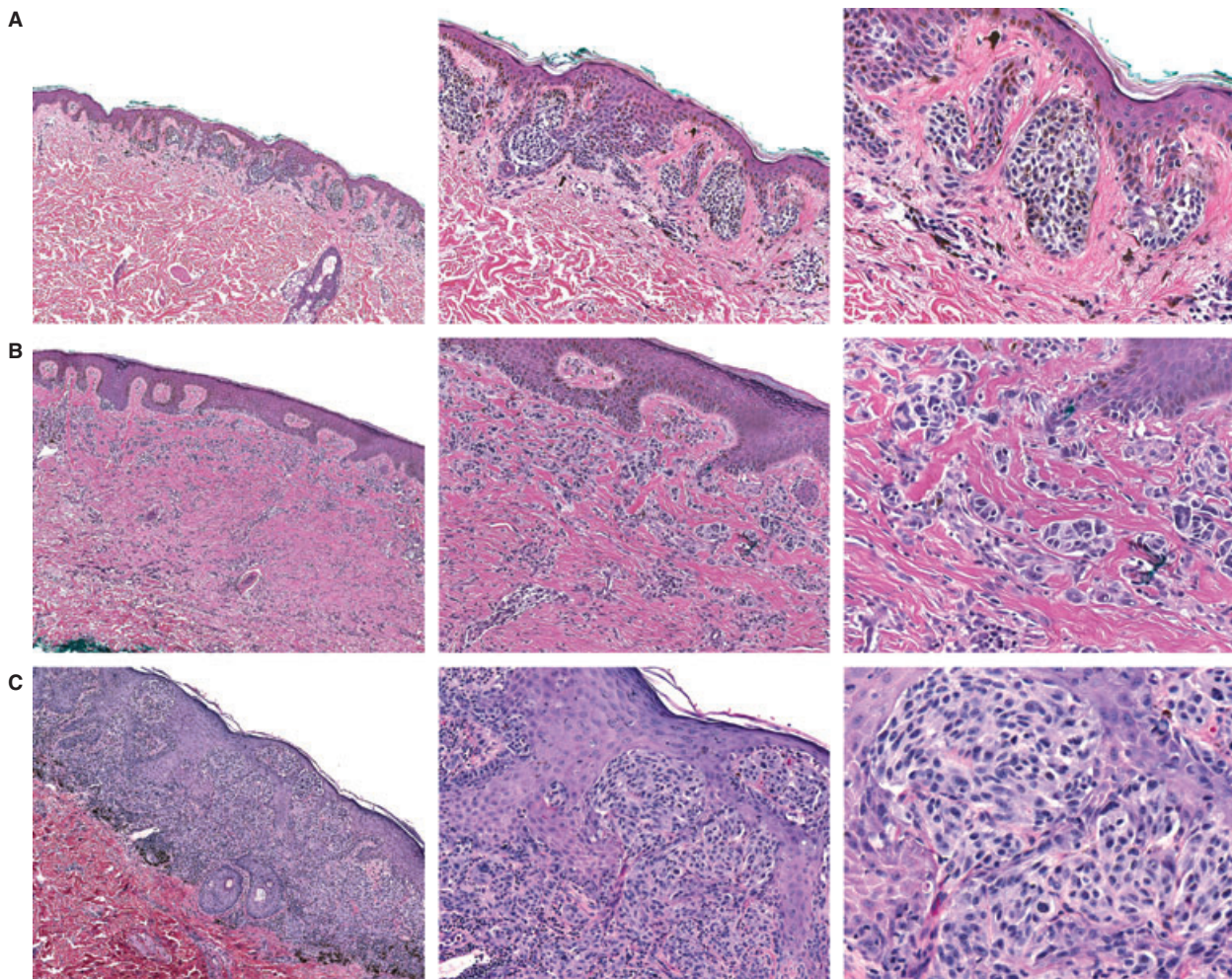


Figure 1. Scanning, intermediate and high-power images of mildly dysplastic naevus (A), severely dysplastic naevus (B) and superficial spreading melanoma (C).

pathologist can assess simultaneously dozens if not hundreds of characteristics of a given slide. In order to approximate the human mind, a computer would need to analyse and assess many characteristics of an image and use the composite of this assessment to justify an outcome.¹¹ Our goal is not to replace the pathologist, but to help the pathologist understand what he or she is seeing and also to set a foundation for future endeavours.

Materials and methods

CASE SELECTION AND ANNOTATION

This study was based on a series of 49 haematoxylin and eosin-stained slides representing different types of melanocytic lesions. Specifically, of malignant lesions (melanoma), 12 slides represented superficial spreading melanoma, four lentigo maligna melanoma and five a combination of other types of melanoma. Of benign lesions, 11 slides represented conventional

naevi, 10 mildly dysplastic naevi and eight severely dysplastic naevi. These slides were chosen by the groups' dermatopathologist (J.W.) from cases seen at University of North Carolina at Chapel Hill (UNC-CH) hospitals. Figure 1 shows examples of a mildly dysplastic naevi (A), severely dysplastic naevi (B) and superficial spreading melanoma (C). Slides were scanned digitally using Aperio ScanScope. Our dermatopathologist then annotated melanocytic cell groups in each image using Aperio Virtual Slide-viewing software. 'Groups', in this context, is used to signify collections of multiple melanocytes, often in nests, with little intervening stroma and without a significant component of other cell types (lymphocytes, etc.). Melanocytic groups were annotated near the dermo-epidermal junction or superficial dermis of conventional and dysplastic naevi. Melanoma cell groups were chosen which were thought to be representative of the lesion. The outcome was 113 groups of superficial spreading melanoma, 37 groups of lentigo maligna melanoma and 40 groups repre-

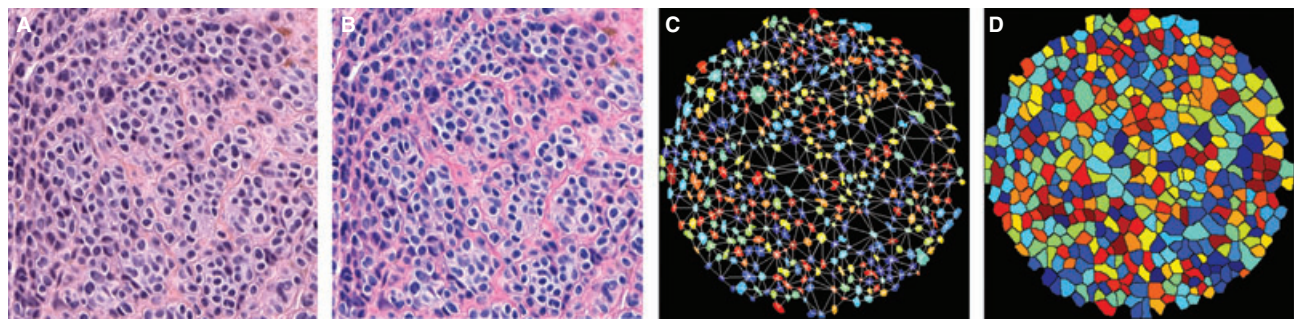


Figure 2. High power images of original hematoxylin and eosin stained groups of benign melanocytic cells were scanned into Aperio ScanScope (A). All groups underwent a standardization stage to account for differences in staining between slides (B). Images were digitally analyzed and features extracted. An example readily shows such features as calculated nuclear area (referred to as area) and Delaunay triangulation, values which both tended to be larger in melanoma than in naevi (C). An approximation for whole cell borders (referred to as region) was also used (D). Many more features were also analysed.

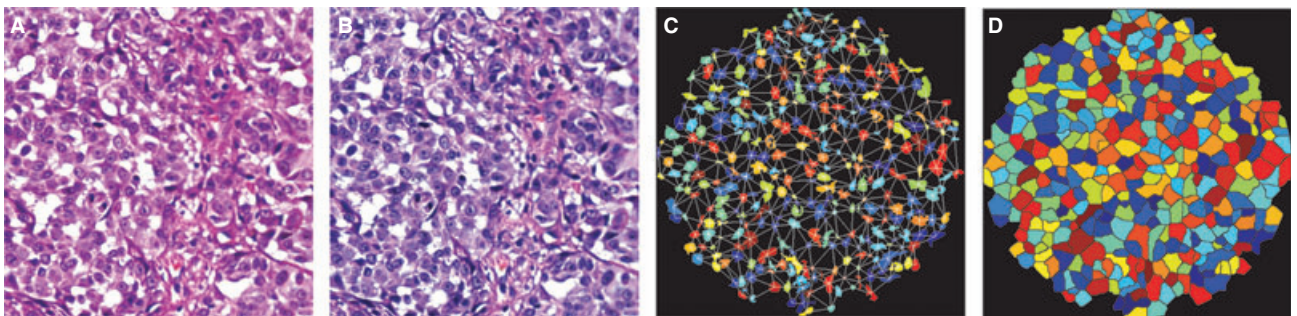


Figure 3. High power images of original hematoxylin and eosin stained groups of malignant melanoma cells were scanned into Aperio ScanScope (A). All groups underwent a standardization stage to account for differences in staining between slides (B). Images were digitally analyzed and features extracted. An example readily shows such features as calculated nuclear area (referred to as area) and Delaunay triangulation, values which both tended to be larger in melanoma than in naevi (C). An approximation for whole cell borders (referred to as region) was also used (D). Many more features were also analysed.

Table 1. Features examined during image analysis. For each feature, the full population was transformed individually as appropriate to make distributions approximately standard Gaussian. Features were summarized over each group using both the mean and standard deviations of 31 features resulting in a total of 62 values or features

1. Area
2. Hu 1
3. Hu 2
4. Hu 3
5. Hu 4
6. Perimeter ratio
7. Region area ratio
8. Eccentricity
9. Rotation
10. Ellipseness
11. Convexity
12. Gabor feature stain 1 scale 5
13: Gabor feature stain 1 scale 10
14. Gabor feature stain 1 scale 20
15. Gabor feature stain 2 scale 5
16. Gabor feature stain 2 scale 10
17. Gabor feature stain 2 scale 20
18. Mean stain 1
19. Mean stain 2
20. Mean residual
21. SD stain 1
22. SD stain 2
23. SD residual
24. Region mean stain 1
25. Region mean stain 2
26. Region mean residual
27. Region SD stain 1
28. Region SD stain 2
29. Region SD residual
30. Mean Delaunay
31. Maximum Delaunay

SD, Standard deviation.

Table 2. A short description of features analysed is provided. Several of these features have been used or described elsewhere. Area is indicative of an approximated nucleus while region is indicative of an approximated whole cell

<i>Nuclear area</i>
<i>Perimeter ratio</i> (defined as the ratio between nuclear boundary length and the square root of the nuclear area, used to measure boundary irregularities)
<i>Region area ratio</i> (the ratio of the area of the nucleus and the area of the surrounding Voronoi cell, used to measure nuclear density)
<i>Eccentricity</i> (the eccentricity of the best-fitting ellipse to a nucleus, defined as $\sin[\text{acos}(b/a)]$, where b is the length of the minor and a the length of the major half-axis of the ellipse)
<i>Rotation</i> of the ellipse (to assess directionality of nuclei)
<i>Ellipseness</i> (deviation in percent of nuclear shape from the best-fitting ellipse shape relative to the nuclear area, as a region-based measure of nuclear irregularity)
<i>Convexity</i> (deviation in percentage of the convex hull of the nuclear shape from the nuclear shape relative to nuclear area) and the Hu moment invariants ¹⁶ of the nuclei as nuclear geometric features
Further, we use the means and standard deviations of the intensities of the haematoxylin stain (stain 1), the eosin stain (stain 2) and the stain residual of the nuclei and their whole cell regions as colour features
<i>Texture</i> is assessed by Gabor features ^{14,15} (evaluated at three spatial scales and for eight orientations) for the haematoxylin and eosin stains
<i>Delaunay</i> – average of line in triangulation ^{14,15}
We further compute the mean and the maximum edge-length of the Delaunay triangulation

senting a combination of other types of melanoma. We annotated 99 groups of conventional naevi, 59 groups of mildly dysplastic naevi and 54 groups of severely dysplastic naevi. Therefore altogether we examined 190 groups of melanoma and 212 groups of naevi (49 slides, 402 groups or annotated areas of melanocytic lesions). The study was approved by the internal review board (IRB) of UNC-CH.

STANDARDIZATION

Prior to image analysis, the images were standardized to account for differences in staining intensity and stain fading over time (Figures 2 and 3). This was accom-

plished through mathematical techniques developed by our group, which used stain vector variation correction, and eliminated secondary differences in stain intensity due to different stains, manufacturers, procedures and storage time.^{12,13}

FEATURE EXTRACTION

Once standardized, images were analysed digitally in order to extract features. We developed software to segment the nuclei (approximations are referred to as 'area') and to provide a proxy for cell borders (known as 'region') for both benign and malignant cell types (Figures 2 and 3). Thirty-one quantitative features were then identified. For each feature, the full population was transformed individually as appropriate to make distributions approximately standard Gaussian. Features were summarized over each group using both the mean and standard deviations of 31 features, resulting in a total of 62 values or features (Table 1, descriptions in Table 2). We refer the reader elsewhere for a description of the Gabor (texture quantification) and Delaunay (based on distances between nuclear centres) features,^{14,15} as well as Hu moment invariants (which capture aspects of nuclear shape).¹⁶

STATISTICAL ANALYSIS

Once data for each of these characteristics were collected, they were analysed statistically using DiProPerm analysis. DiProPerm is a non-parametric hypothesis test that is especially well suited to high-dimensional data. In this analysis, we use DiProPerm to test the null hypothesis of equal group means. Our initial comparison, chosen *a priori*, was that of all melanoma to all naevi. We also explored approximately 20 pairwise comparisons between different melanoma versus naevus subtypes. We used a Bonferroni adjustment for multiple comparisons. Four pertinent pathological contexts were then chosen for explicit discussion, as follows.

- 1 Comparison of all melanoma versus all types of naevi.
- 2 Comparison of melanoma World Health Organization (WHO) subtypes to all types of naevi.
- 3 Comparison of lesions classified as severely dysplastic naevi to all other naevi subtypes, including conventional naevi and mildly dysplastic naevi.
- 4 Comparison of all melanoma to severely dysplastic naevi.

In each of these contexts we measured the degree of separation using the receiver operating characteristic (ROC) area, assessed statistical significance using the DiProPerm *P*-value, and identified which features drove each separation.

Results

During data analysis regarding all melanoma versus all naevi, we found that the histological features which drove the separation between these two subsets were nuclear area, mean Delaunay, convexity and perimeter ratio (Figure 4A). All these values were larger in melanoma than in naevi. The ROC area for this context was 0.95, $P < 0.0001$ (Figure 4B).

We found that dividing melanoma into subtypes produced even greater separation. ROC area for superficial spreading melanoma versus all naevi was 0.98, $P < 0.0001$. The ROC area for lentigo maligna melanoma versus all naevi was 0.96, $P < 0.0001$. Finally, the ROC area for all other types of melanoma versus all naevi was 0.99, $P < 0.0001$.

We also compared severely dysplastic naevi to all other types of naevi. We found that separation of these two data subtypes was driven by differences in the standard deviation of calculated whole cell eosin staining intensities (less in severely dysplastic naevi versus others), average whole cell eosin staining intensities, standard deviation of haematoxylin staining in each whole cell and mean nuclear area (we called these standard region mean stain 2, mean region mean stain 2, mean region standard stain 1 and mean area; Figure 5A). All these values except the first, standard region mean stain, were greater in severely dysplastic naevi. The ROC area for these data was 0.84, $P < 0.0001$ (Figure 5B).

We compared all melanoma to severely dysplastic naevi. We found that separation of these lesions was driven by approximated shape features (mean Delaunay, convexity), nuclear eosin staining (mean stain 2) and a nuclear textural feature (mean Gabor stain 1). All these features were greater in melanoma than in severely dysplastic naevi except for mean Gabor stain 1 (Figure 6A). The ROC area for these data was 0.95, $P < 0.0001$ (Figure 6B).

Discussions/Conclusions

During our analysis we found that the features which best separated malignant melanoma from naevi were as follows.

- 1 Mean area nuclear area; greater in melanoma.
- 2 Mean Delaunay (the mean edge length of a triangulation based on the cell centres); greater in melanoma.
- 3 Mean convexity (a measure of the convexity of the segmented nucleus); greater in melanoma.
- 4 Mean perimeter ratio [the ratio of the length of the nuclear perimeter to the square root of the area (nuclear) which indicates irregularity of nuclear boundary]; greater in melanoma.

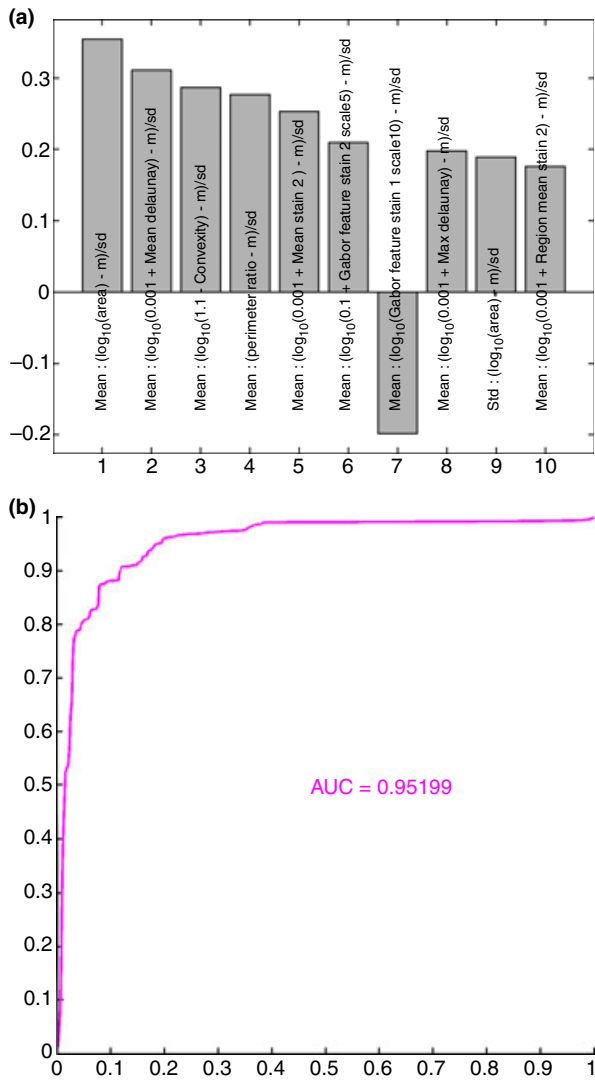


Figure 4. A, These features were most useful in driving the separation of melanoma from naevi. While the name provided on the bar also indicates statistical transformation, the top four features represent nuclear area, mean Delaunay, convexity and perimeter ratio (top 10 features are shown). B, Area under the receiver operator characteristic (ROC) curve of 0.95, $P < 0.0001$.

Further, we found that this separation was improved by dividing melanoma into subtypes. Each subtype of melanoma had a larger ROC area when compared to naevi than when all melanomas were included together. Features that best differentiated severely dysplastic naevi from other naevi and mildly dysplastic naevi were as follows.

1 Standard region mean stain 2 (differences in eosin staining intensities between whole cell regions). We found that severely dysplastic naevi demonstrated less variability, i.e. lower standard deviation, in whole cellular eosin staining than other types.

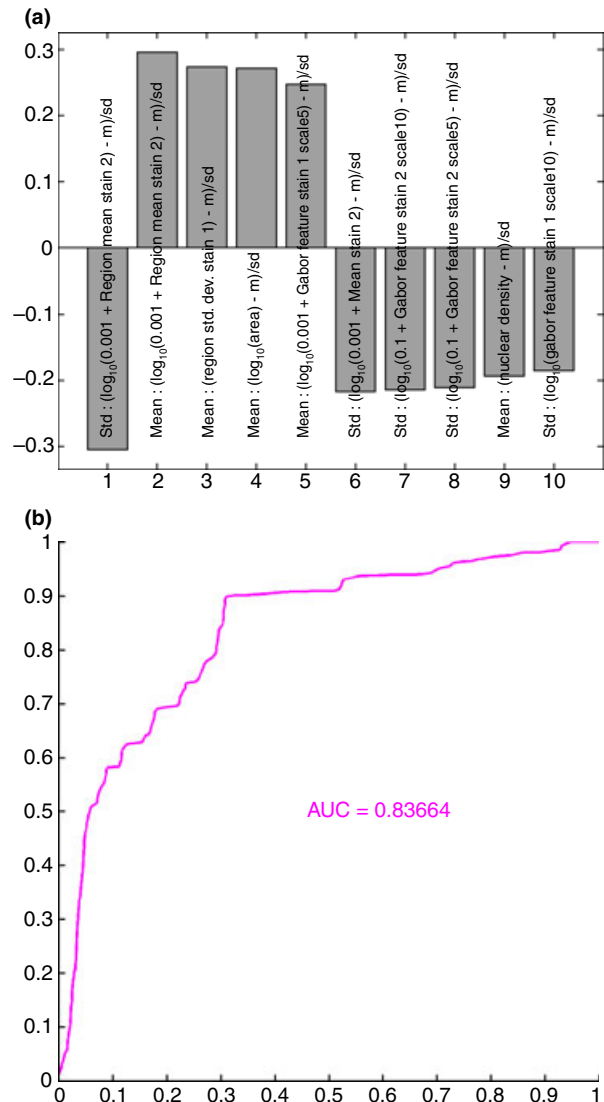


Figure 5. A, These features were most useful in driving the separation of severely dysplastic naevi from other types of naevi. While the name provided on the bar also indicates statistical transformation, the top four features represent differences in the standard deviation of calculated whole cell eosin staining intensities (calculated whole cell called 'region' and staining differences are less in severely dysplastic naevi than in others), average eosin staining intensities, average standard deviation of haematoxylin nuclear staining in each nuclei (calculated nuclei is called 'area') and mean nuclear area. B, Area under the receiver operator characteristic (ROC) curve of 0.84, $P < 0.0001$.

2 Mean region mean stain 2 (mean eosin staining intensities of the region). We found that severely dysplastic naevi demonstrated greater average eosin staining of the approximated whole cell region than other types of naevi.

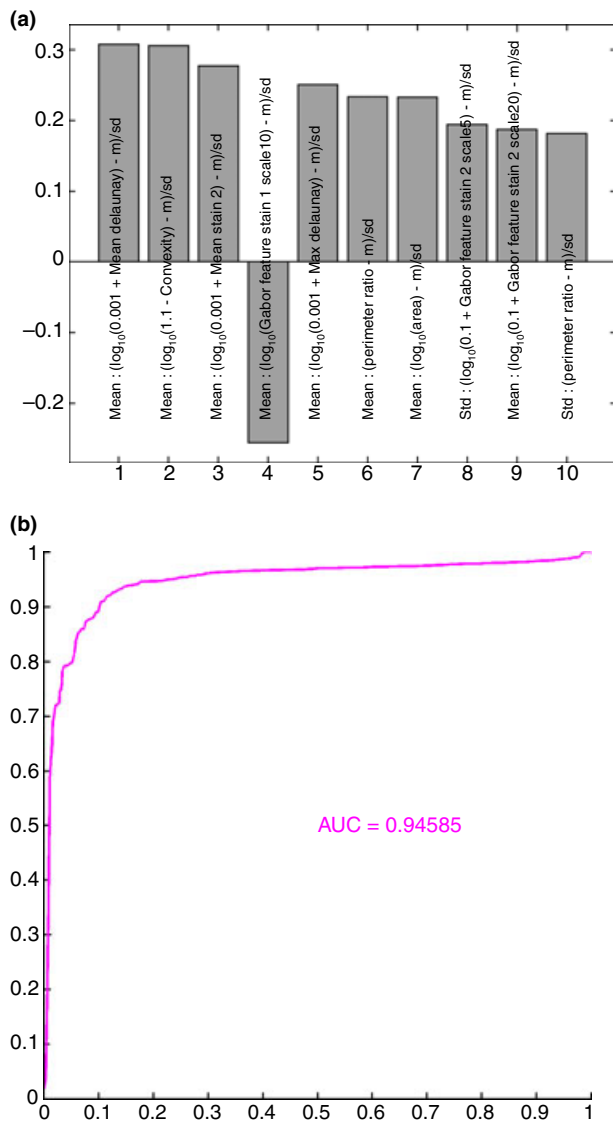


Figure 6. A, These features were most useful in driving the separation of melanoma from severely dysplastic naevi. While the name provided on the bar also indicates statistical transformation, the top four features represent approximated shape features (mean Delaunay, convexity), nuclear eosin staining (mean stain 2) and a nuclear textural feature (mean Gabor stain 1). The top 10 features are shown. B, Area under the receiver operator characteristics (ROC) curve of 0.95, $P < 0.0001$.

3 Mean region standard stain 1 (the larger this value, the more haematoxylin staining variability there is in the whole cell region of each cell in that type of lesion). This value was greater in severely dysplastic naevi.

4 Mean area (nuclear area) was greater in severely dysplastic naevi.

Finally, separation of melanoma from severely dysplastic naevi was driven by the following.

- 1 Mean Delaunay (the mean edge length of a triangulation based on the cell centres); greater in melanoma.
- 2 Mean convexity (a measure of the convexity of the segmented nucleus); greater in melanoma.
- 3 Mean stain 2 (mean eosin staining intensities of the area). We found that melanoma demonstrated greater average eosin staining of the area (approximated nuclei) than severely dysplastic naevi.
- 4 Mean Gabor stain 1 (textural differences of the nuclei) was greater in severely dysplastic naevi and also drove separation of these two entities.

Of course, while the features listed above drove separation of these lesion types most significantly, true separation and hence ROC areas were derived from a composite of all features. It might have been hoped that one dominant feature would be adequate to classify lesions; however, this is not the case. In fact, many features are needed for effective separation and are accounted for in our method.

Some of our results confirm intuitive expectations. For example, mean nuclear area, mean Delaunay, mean convexity and mean perimeter ratio being greater in melanoma compared with naevi is very reasonable and correlates with the subjective experience of the pathologist in comparing many melanomas to benign lesions. The separation we obtained between individual melanoma subtypes and naevi, which was greater than when we included all melanomas together as a whole, also seems natural. This is because slightly different features may drive the traditional diagnosis of melanoma subtypes⁶ which, when taken in aggregate, diminish the strength of any one feature.

Our analysis regarding the separation of severely dysplastic from other naevi reveals properties which are more difficult for the pathologist to assess visually: we found the standard deviation of staining intensities and average staining intensities to be significant driving forces, while more easily conceptualized features such as standard deviation of area and mean nuclear area played a secondary role. Conversely, the long-standing disagreement over dysplastic naevi cytology may be related to the fact that these important features are difficult to assess visually. What is unique about our analysis is that we need not rely on any one feature to separate these lesions independently; instead, we are using 62 features simultaneously to allow the greatest distinction possible. This is of major importance, and a significant difference between our study and previous cytometric analyses.

An objective method of differentiating melanoma from severely dysplastic naevi may aid clinical management. We found that these two entities were

separated by calculated shape features (mean Delaunay, convexity, greater in melanoma) and by features approximating nuclear eosin staining (mean stain 2) and texture (mean Gabor stain 1, greater in dysplastic naevi). Moreover, combining all 62 features yields powerful separation ($P < 0.0001$).

Relatively few studies have attempted this level of analysis of melanocytic lesions. Several papers have used image analysis to clarify the debate regarding the presence or absence of cytological atypia in dysplastic naevi. A 1990 paper¹⁷ contributed to the discussion of whether dysplastic naevi exhibit cytological changes by looking at four morphological characteristics: nuclear area, standard deviation of nuclear area, nuclear roundness, standard deviation of nuclear roundness. They found the latter three features to be significantly greater for dysplastic naevi than for conventional naevi. They also found that melanoma differed significantly from dysplastic naevi in mean nuclear area, standard deviation of nuclear area, mean ploidy and standard deviation of ploidy.¹⁷ While their paper used different methods to examine different characteristics, it is interesting to compare their principal findings with ours. One of these findings was that the nuclear area was greater in melanoma than in naevi, which was consistent with our results. This group also compared melanoma to dysplastic naevi and found that mean nuclear area and standard deviation of nuclear area were significantly greater for melanoma than dysplastic naevi. In our study, we found that the greatest factor differentiating melanoma from all types of naevi was mean nuclear area, and that standard deviation of nuclear area played a significant but secondary role. Other investigators have also found that mean nuclear area is greater for melanoma and severely dysplastic naevi than other types of naevi.¹⁸ Another paper emphasized the importance of texture in the evaluation of melanocytic lesions.¹⁹ Textural features are subtle and are often emphasized less than other characteristics; however, we also utilized texture (measured by standard deviation of stain as well as Gabor features in our analysis), and found that it was important in helping to drive the separation of categories.

Despite differences in design, set-up and goals making direct comparison difficult, our major findings are largely consistent with these earlier reports, which we have built upon and taken in novel directions. In particular, our analysis is strengthened by the use of new and sophisticated colour normalization/standardization techniques with advanced statistical and computational techniques that examine many features not previously evaluated.

Our study has a number of limitations. For example, we use a data set that focuses on cytological rather than architectural features. It is widely recognized that architectural features are important for the diagnosis and differentiation of benign from dysplastic naevi from malignant melanoma. In many cases, architectural features may outweigh cytological differences. A second caveat to our analysis is that the features that we have highlighted as being important differences between these types of lesions are strictly those that the computer views as being important, and that a pathologist looking at the lesions would see these features only subconsciously, or not at all. This is especially true for less intuitive features, such as standard deviation of staining intensities. Thirdly, it is well known that melanoma can take on a variety of types, and we have selected several more common types to use in our analysis. Some of the most difficult diagnostic dilemmas occur when examining Spitz or Spitzoid lesions, that our study does not include. However, the comparisons we made with more typical lesions were strongly statistically significant. We think that Spitzoid lesions and other less common presentations would be an interesting area of study for the future; however, for this study we chose to focus on lesions of indisputable diagnosis. One final important caveat is that while there is generally little ambiguity between melanoma versus conventional naevi, there are more differences of opinion when grading dysplastic naevi into mild and severe. While the diagnosis of dysplastic naevi can, in most cases, be made architecturally, we cannot rule out the notion that during the grading process other pathologists might not have subcategorized the lesions exactly as we did, thereby adding a minimal level of subjectivity to the results of our third comparison.

In ordinary life, we are used to thinking in three dimensions. In considering our data, we analyse it in 62 dimensions, with each dimension being an image feature. We are then able to take all these features in composite to analyse the data most clearly. In our current application we are looking to separate melanoma from naevi and dysplastic naevi from conventional and mildly dysplastic naevi. One might hope for a single 'magic bullet' feature that would give 100% separation between groups of melanocytic entities. Unfortunately, this does not exist. Instead, a composite of multiple features provides the best separation. Computational analysis allows for the comparison of multiple features to obtain a substantial degree of separation.

With increasing technology and better software, the application of this type of analysis becomes increasingly

practical and it follows that the use of digital analysis to aid in the interpretation of histological images is an aspect of pathology that should increase in the future. This motivates the need to study, improve and explore such analysis. Our study is unique in its utilization of sophisticated methods to study melanocytic histology and provides a foundation for future studies.

Digital imaging may be used to help predict prognosis, as has been reported with regard to renal and bladder cancers.^{20,21} Work is currently being conducted to improve the traditional classification of melanoma by forming subgroups that are genetically more homogeneous and therefore more significant from a bench and clinical viewpoint.^{22,23} Much of the recent research in melanoma has gravitated towards using specific drugs for lesions with specific mutations,²⁴ and it is hoped this approach may provide therapeutic benefit and improve survival. It is possible that image analysis could help in the prediction of mutation status. Using the experience we have gained during this analysis, these are concepts we hope to explore in the future.

Acknowledgement

This work was supported, in part, by the University Cancer Research Fund, Lineberger Comprehensive Cancer Center, University of North Carolina, Chapel Hill, NC, CA112243, CA11243-05S109 and P3OES010126. Susan Wei was supported by an NSF Graduate Fellowship and NIH Predoctoral Training Program in Bioinformatics and Computational Biology, T32 GM067553-05S1. Marc Niethammer was supported by NIH NIBIB 5P41EB002025-27.

References

1. Cho YR, Chiang MP. Epidemiology, staging (new system), and prognosis of cutaneous melanoma. *Clin. Plast. Surg.* 2010; **37**: 47–53.
2. Fleming MG. Pigmented lesion pathology: what you should expect from your pathologist, and what your pathologist should expect from you. *Clin. Plast. Surg.* 2010; **37**: 1–20.
3. Troxel DB. Medicolegal aspects of error in pathology. *Arch. Pathol. Lab. Med.* 2006; **130**: 617–619.
4. Culpepper KS, Granter SR, McKee PH. My approach to atypical melanocytic lesions. *J. Clin. Pathol.* 2004; **57**: 1121–1131.
5. Zembowicz A, Ahmad A, Lyle SR. A comprehensive analysis of a web-based dermatopathology second opinion consultation practice. *Arch. Pathol. Lab. Med.* 2011; **135**: 379–383.
6. Smoller BR. Histologic criteria for diagnosing primary cutaneous malignant melanoma. *Mod. Pathol.* 2006; **19**(Suppl. 2): S34–S40.
7. Friedman RJ, Farber MJ, Warycha MA, Papathasis N, Miller MK, Heilman ER. The 'dysplastic' nevus. *Clin. Dermatol.* 2009; **27**: 103–115.
8. Hollander AW. Development of dermatopathology and Paul Gerson Unna. *J. Am. Acad. Dermatol.* 1986; **15**: 727–734.
9. Weyers WA. Bernard Ackerman – the 'Legend' turns 70. *J. Am. Acad. Dermatol.* 2009; **60**: 525–529.
10. Hatanaka Y, Hashizume K, Nitta K, Kato T, Itoh I, Tani Y. Cytometrical image analysis for immunohistochemical hormone receptor status in breast carcinomas. *Pathol. Int.* 2003; **53**: 693–699.
11. Gil J, Wu H-S. Applications of image analysis to anatomic pathology: realities and promises. *Cancer Invest.* 2003; **21**: 950–959.
12. Macenko M, Niethammer M, Marron JS et al. A method for normalizing histology slides for quantitative analysis. *Proc. Int. Symp. Biomed. Imaging (ISBI)* 2009; 1107–1110.
13. Niethammer M, Borland D, Marron J, Woolsey J, Thomas NE. Appearance normalization of histology slides. *Lecture Notes in Computer Science, Machine Learning in Medical Imaging* 2010; **6357**: 58–66.
14. Doyle S, Hwang M, Shah K, Madabhushi A, Feldman M, Tomaszewski J. Automated grading of prostate cancer using architectural and textural image features. *Biomedical imaging: from nano to macro*. ISBI 2007. 4th IEEE International Symposium, 2007; 1284–1287.
15. Doyle S, Madabhushi A, Feldman M, Tomaszewski J. A boosting cascade for automated detection of prostate cancer from digitized histology. *Med. Image Comput. Comput. Assist. Interv.* 2006; **9**: 504–511.
16. Ming-Kuei Hu. Visual pattern recognition by moment invariants. *IEEE Trans. Inform. Theory* 1962; **8**: 179–187.
17. Fleming MG, Wied GL, Dytch HE. Image analysis cytometry of dysplastic nevi. *J. Invest. Dermatol.* 1990; **95**: 287–291.
18. Bruijn JA, Berwick M, Mihm MC Jr, Barnhill RL. Common acquired melanocytic nevi, dysplastic melanocytic nevi and malignant melanomas: an image analysis cytometric study. *J. Cutan. Pathol.* 1993; **20**: 121–125.
19. Fleming MG, Friedman RJ. Multiparametric image cytometry of nevi and melanomas. *Am. J. Dermatopathol.* 1993; **15**: 106–113.
20. Carducci MA, Piantadosi S, Pound CR et al. Nuclear morphometry adds significant prognostic information to stage and grade for renal cell carcinoma. *Urology* 1999; **53**: 44–49.
21. Blomjous CE, Vos W, Schipper NW et al. The prognostic significance of selective nuclear morphometry in urinary bladder carcinoma. *Hum. Pathol.* 1990; **21**: 409–413.
22. Broekert SMC, Roy R, Okamoto I et al. Genetic and morphologic features for melanoma classification. *Pigment Cell Melanoma Res.* 2010; **23**: 763–770.
23. Curtin JA, Fridlyand J, Kageshita T et al. Distinct sets of genetic alterations in melanoma. *N. Engl. J. Med.* 2005; **353**: 2135–2147.
24. Flaherty KT, Hodi FS, Bastian BC. Mutation-driven drug development in melanoma. *Curr. Opin. Oncol.* 2010; **22**: 178–183.